Lecture 7: Stability of RCE and Rotating RCE

Kerry Emanuel; notes by Alexis Kaminski and Shineng Hu

June 24

1 Stability of RCE

The radiative moist convective equilibrium (RCE) state we have been considering so far is evidently unstable in some conditions. By considering the linear stability of the RCE state (recalling that RCE is a statistical equilibrium), is it possible to explain the clustering seen previously in the cloud-resolving simulations? In order to proceed, some additional concepts must be introduced to allow for dynamics in RCE. In some sense, we will take the opposite approach to classical geophysical fluid dynamics in that the dynamics will be parameterized while the physics will be resolved.

1.1 Weak temperature gradient approximation

As the RCE state considered so far is non-rotating, there is no way to sustain lateral temperature gradients (e.g. $\mathrm{d}T/\mathrm{d}x$). As a result, the weak temperature gradient (WTG) approximation can be made, which assumes that the dynamics operate so as to keep temperature constant in the horizontal [Sobel and Bretherton, 2000].

We can suppose that we have an RCE state and add an SST anomaly, essentially making a small patch of ocean slightly warmer. In this case, the atmosphere wants to be warmer above the SST anomaly, but with the WTG approximation this is not allowed to happen. This results in large-scale ascent above the patch such that adiabatic heat balances the anomaly. In essence, the SST anomaly induces that vertical motion which is necessary to keep the atmosphere relatively cool. The vertical velocity also advects water vapour vertically, leading to a moistening of the column, an increase in clouds, and less sunlight reaching the surface.

The WTG approximation can be extended to a weakly rotating framework. In this case, if w is known from WTG, then the vorticity equation can be used to solve for the horizontal component of motion. This allows us to solve for atmospheric flow without solving the equations of motion, even in a single column model. It should be noted that the convection in the system does not allow the ascending air to reach saturation on the macro scale.

WTG may also be used to empirically determine the stability of the RCE state. A single column model can be run until equilibrium, at which point it is stopped and restarted in WTG mode with a small amount of noise added. If the RCE state is stable, at this point the noise dies away. However, for an unstable RCE state, the noise will lead to ascent or descent throughout the column.

The WTG approximation may also be derived asymptotically by assuming convection and gravity waves act on sufficiently fast timescales (in analogy with the quasigeostrophic approximation) that they are able to smooth out temperature perturbations quickly. Virtual temperature (i.e. temperature corrected for water vapour content) above the planetary boundary layer (PBL) is assumed to be invariant. The vertical velocity w is thus calculated in order to maintain constant virtual temperature, using the vertical motion to advect water vapour.

1.2 Single column model

The model used is the MIT Single-Column model. It employs Fouquart & Bonnel shortwave radiation, Morcrette longwave radiation, Emanuel-Zivkovic-Rothman convection, and the Bony-Emanuel cloud scheme. 25 hPa grid spacing is used in the troposphere, with higher resolution in the stratosphere. The model is run with fixed SST until the RCE state is reached, then re-initialized in WTG mode with fixed temperature at 850 hPa and above to simulate the PBL. Small perturbations in w are added to the initial condition.

When the SST is less than approximately 32°C, there is no drift from the RCE state, and the initial perturbations decay away. However, for higher SSTs, there is a migration toward states with either ascent (formation of a cluster) or descent (formation of a hole), depending on the random initial perturbations. These states correspond to multiple equilibria in 2-column models, observed by Nilsson and Emanuel [1999], Raymond and Zeng [2000] and others.

Figure 1 shows timeseries data, starting from the addition of noise, for the descending branch. Plotted are contours of specific humidity, $\omega = \mathrm{d}p/\mathrm{d}t$ (an analogue for vertical velocity in pressure coordinates, where $\omega \simeq -\rho g w$), radiative heating, and convective heating. Note that the height of the cutoff in data for ω, and the height at which convective heating changes sign, corresponds to the PBL at 850 hPa. Qualitatively, figure 1 shows that in the descending branch air is sinking as the atmosphere is drying out. Radiative cooling is observed low in the troposphere. The growth rate of the formation of the hole (in the case of the descending branch) is similar to that seen in the cloud-resolving model discussed earlier.

Figure 2 shows the effect of an instantaneous, vertically-uniform reduction of the specific humidity by 20% from the RCE state with two different SST values. In the stable case (SST=25°C), the reduced specific humidity leads to a negative shortwave radiation anomaly, as there is less water vapour present to absorb the incoming solar radiation. The longwave radiation anomaly is mostly positive, as less water vapour leads to less radiative cooling by infrared.

However, the unstable case (SST=40°C) exhibits markedly different behaviour. While the shortwave radiation anomaly is similar to that of the stable scenario (indicating reduced absorption of incoming solar radiation), the longwave radiation anomaly is an order of magnitude larger than that of the stable scenario. The longwave radiation anomaly is positive above approximately 750 mbar but negative below. This is a consequence of the nonlocal nature of radiation, with the lower layers receiving less infrared radiation from above. In this circumstance where RCE is very warm, the basic state has large quantities of water vapour and very high emissivity in the lower troposphere, though the emissivity

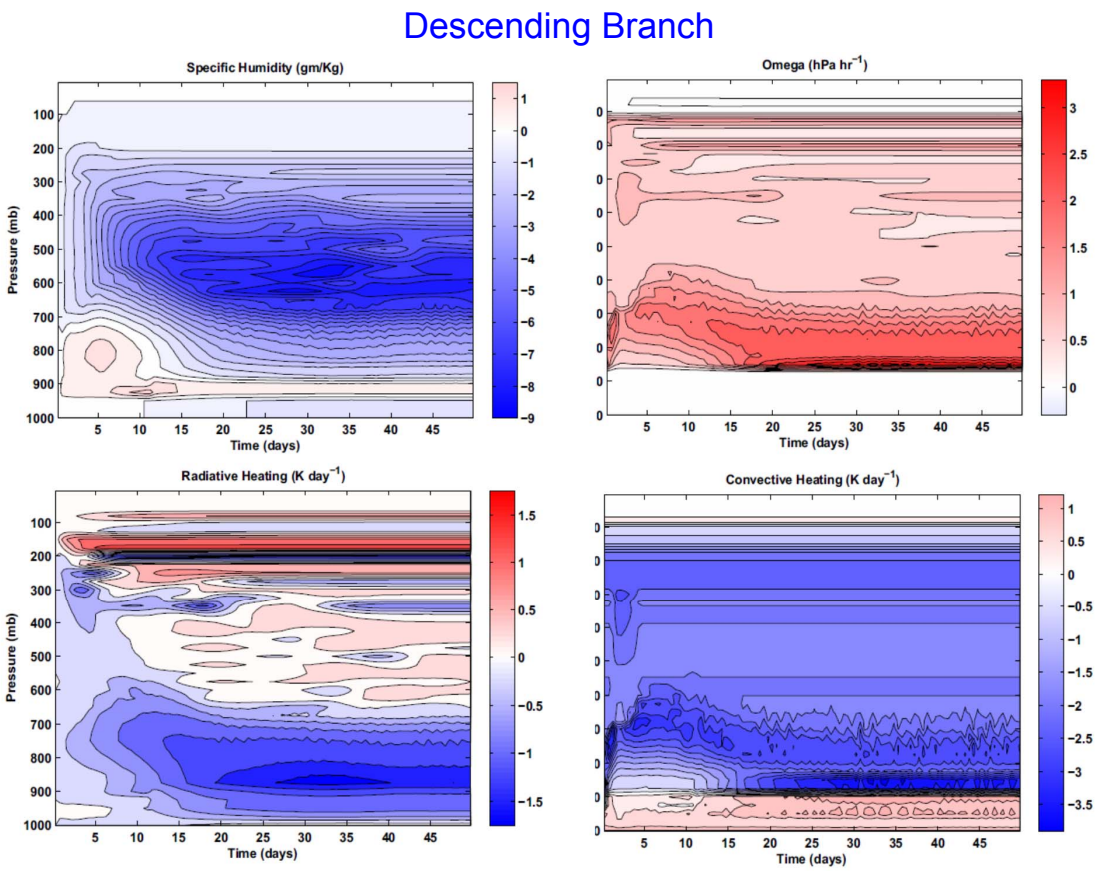

Figure 1: Timeseries contours of specific humidity in gm/kg (top left), ω in hPa hr^{-1} (top right), radiative heating in K day^{-1} (bottom left), and convective heating in K day^{-1} (bottom right) for the descending branch of the WTG single-column model results. From figure 3 of Emanuel et al. [2014].

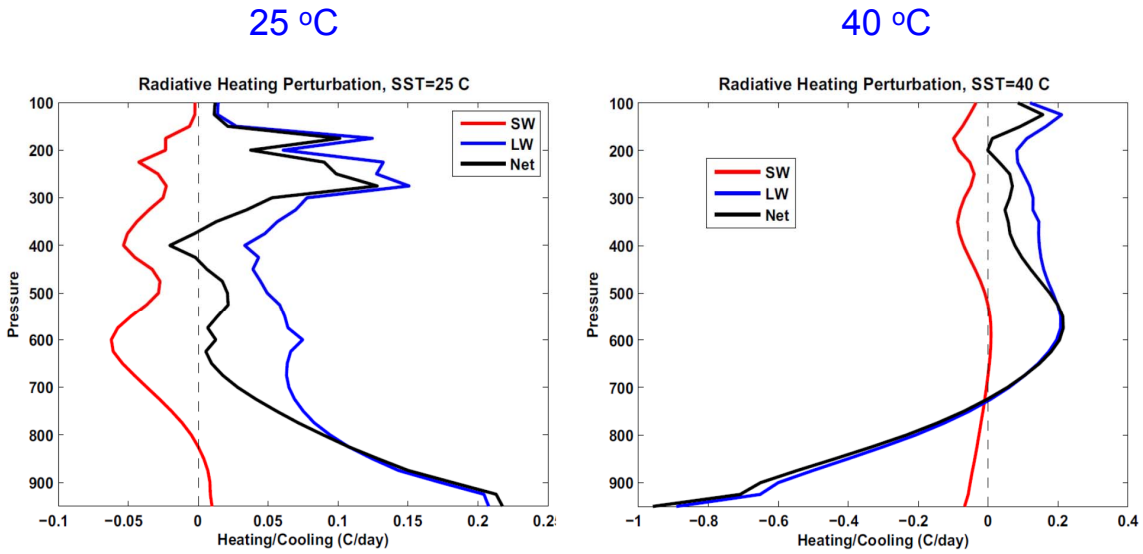

Figure 2: The response of shortwave (SW), longwave (LW), and net perturbation heating rates to an instantaneous reduction in specific humidity for (left) SST = 25° and (right) SST = 40°. From figure 5 of Emanuel et al. [2014].

is not as high in the higher troposphere. The basic state dries: warming occurs locally but emits less radiation to the lower troposphere, which in turn receives less radiation and cools.

Figure 3 shows the net radiation anomaly for the specific humidity perturbation used in figure 2 for a range of SST. A clear qualitative transition is observed between SST values of 30°C and 35°C, corresponding to states above and below the critical SST for stability of approximately 32°C.

The drying of the basic state has consequences for stability, as drying introduces downward motion which further dries in the unstable cases. Convection is also reduced, which dries the upper troposphere and lower stratosphere due to downward flux of water vapour. It should be noted that even if convection shut down entirely in the column, the troposphere would not be expected to dry out entirely as neighbouring columns would be in RCE, leading to horizontal motions bringing in water vapour.

1.3 Two-layer model

The mechanism described above requires at least two troposphere layers to be understood, and cannot be parameterized as Newtonian relaxation. As such, we consider a two-layer troposphere model, shown in figure 4, for which RCE can be calculated and the linear stability of the resulting state can be analyzed.

The critical SST of approximately 30°C can be thought of in terms of the Clausius-Clapeyron equation: the troposphere needs to be sufficiently opaque to longwave radiation, with optical depth increasing with increasing temperature.

The basic state of this system is moist RCE with a grey atmosphere. The temperatures T_1 and T_2 are fixed by the longwave infrared emissivities ε_1 and ε_2, respectively, and the

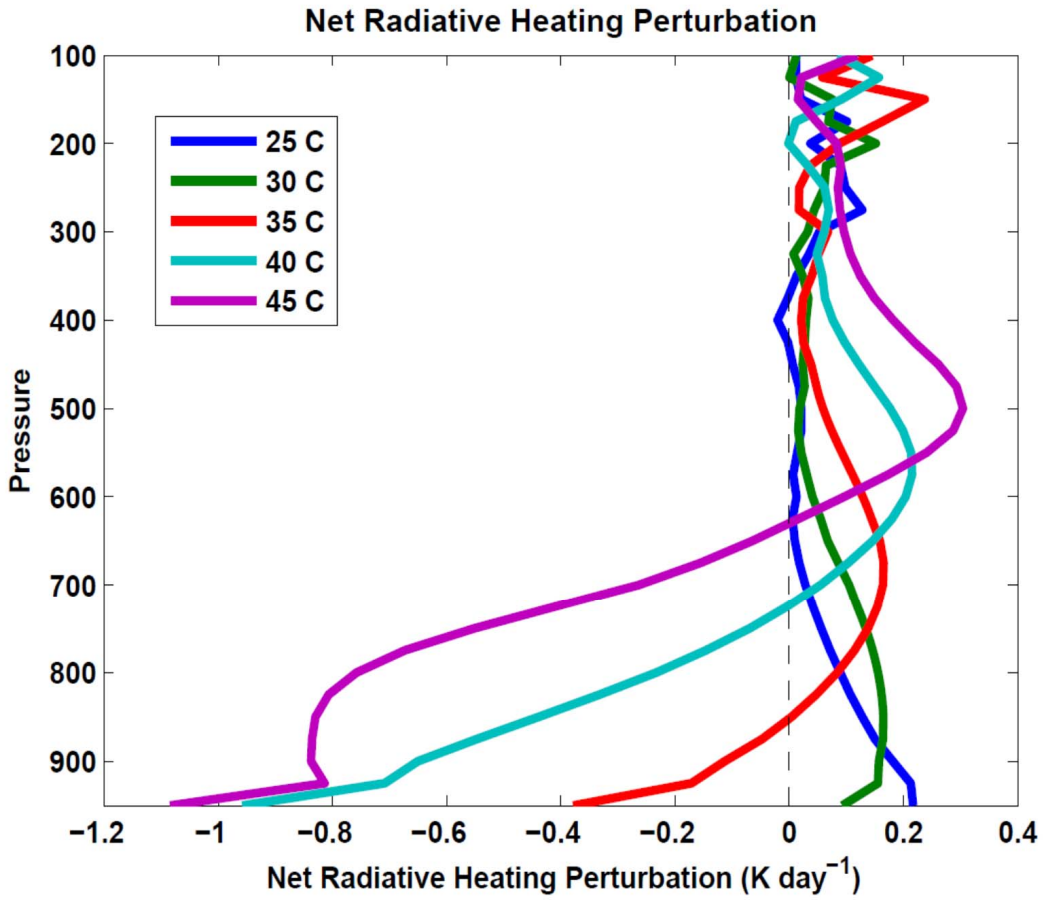

Figure 3: The response of perturbation net heating rates at several SST values to an instantaneous reduction in specific humidity. From figure 6 of Emanuel et al. [2014].

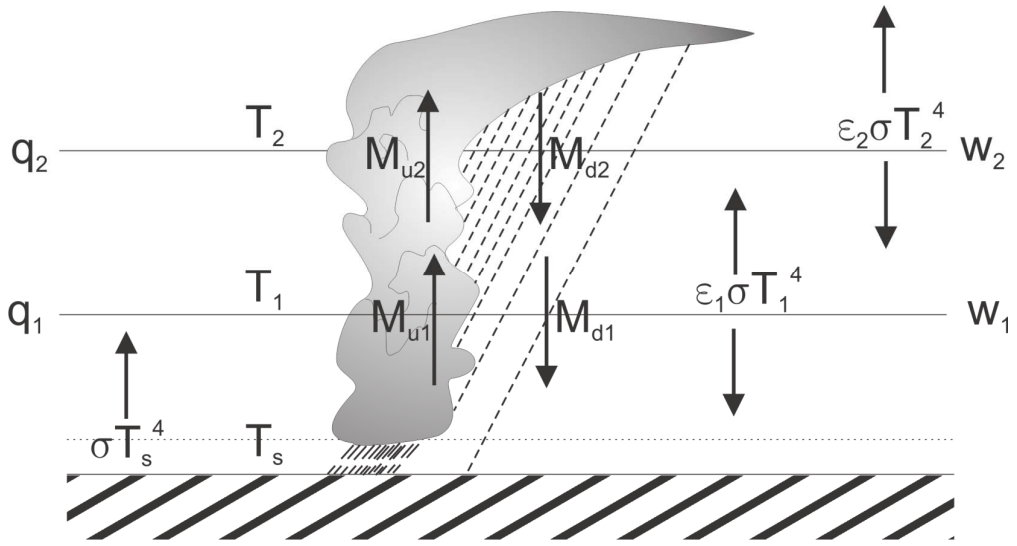

Figure 4: Schematic for the two-layer troposphere model for RCE stability. From figure 1 of Emanuel et al. [2014].

surface temperature is specified. The water vapour-dependent emissivities are controlled by q_1 and q_2, which are the only time-dependent quantities in the model. The boundary layer is held in quasi-equilibrium, with the convective mass fluxes M calculated such that the enthalpy of the boundary layer is held fixed in time, and the vertical velocities w are calculated from WTG [Emanuel et al., 2014].

As seen in the cloud-resolving model, the resulting structure is independent of any horizontal scale, and the scale of the self-aggregating patches appears to increase with the domain size. The physics do not explain the scale of the patches. One possible mechanism by which the size of the clusters may be set is related to the convective turbulence of the surroundings. Convective clouds have an order one aspect ratio and a well-defined horizontal length scale, which can be used to establish a scale for the turbulent diffusion. The vertical velocities associated with convective turbulence, though unsolved, are $\mathcal{O}(\mathrm{m/s})$, and the vertical scale of the clouds does not change much. If we let H be the scale of the clouds and v_c be the characteristic velocity, then the turbulent diffusivity scales like $v_c H$. The descent of air in a patch acts to dry the column; conversely, the turbulence is acting to remoisten the patch. For air descending in a patch of size L with velocity w, the ratio of drying to moistening can be scaled as $(wH)/(v_c L)$. So, for small holes, turbulent diffusion is relatively more influential, and making the domain large is equivalent to decreasing the effect of the turbulent diffusion on the formation of the holes. This may explain why larger domain sizes were needed to see patches in the cloud-resolving models for higher SSTs. This mechanism gives a lower bound of sorts on the required size of the patches, but does not provide an upper bound.

Based on this model, a criterion for instability is

$$\frac{\overline{\dot{Q}_1}}{\varepsilon_1}\frac{\partial \varepsilon_1}{\partial q_1} + (1-\varepsilon_p)\frac{\overline{\dot{Q}_2}}{\varepsilon_2}\frac{\partial \varepsilon_2}{\partial q_2} + \varepsilon_p \frac{S_2}{S_1}\frac{\sigma \varepsilon_1 T_2^4}{\rho_1}\frac{\partial \varepsilon_2}{\partial q_2} > 0\,, \tag{1}$$

where $\varepsilon_{1,2}$ are emissivities, $\dot{Q}$ is the radiative heating per unit mass, S_2/S_1 is the $\mathcal{O}(1)$ ratio of dry static stabilities, and ε_p is the precipitation efficiency with typical values $0.5 < \varepsilon_p < 1$. Convection produces downdrafts driven by precipitation; $\varepsilon_p = 0$ corresponds to all precipitation re-evaporating leading to no heating, while $\varepsilon_p = 0$ corresponds to no re-evaporation and no downdrafts.

In (1), the first term is negative but small when atmospheric moisture is low. The second term is negative but not necessarily small. It is only the third term which is positive, and instability only occurs if this term is sufficiently large. The resulting instability is radiatively driven due to the dependence of the emissivities $\varepsilon_{1,2}$ on water vapour and convection: RCE becomes linearly unstable if the infrared opacity of the lower troposphere is sufficiently large and if ε_p is large.

We can consider ordinary RCE, as seen in the top row of figure 5 and perturb locally with downward vertical velocity. For low SST, i.e. when the system is stable, the shortwave radiative heating is not strongly affected, while longwave radiative cooling is reduced throughout the column. The convective heating is also somewhat reduced. The net result is positive perturbation heating, leading to large scale ascent through WTG and negative feedback on the initial downward perturbation, as shown in the middle row of figure 5.

However, for high SST (shown in the bottom row of figure 5), the downward vertical velocity perturbation leads to strong negative perturbations in the shortwave heating. Longwave radiative cooling is reduced in the upper troposphere, rather than throughout the column, as the change in optical depth in the lower troposphere due to the velocity perturbation is very small. The longwave cooling of the lower troposphere is increased, and convective heating is decreased. The net result is thus negative perturbation heating which, as a consequence of WTG, induces large scale descent, and as such acts as a positive feedback on the initial downward perturbation.

When the resulting instability becomes nonlinear, cloud effects on radiation begin to take over. These effects are dominant once a cluster has formed, as the central dense overcast causes an intense anomaly in outgoing longwave radiation. However, it should be emphasized that cloud feedbacks are not important for instigating instability, but maintain the clusters when already formed; there is a strong hysteresis in the RCE system. Figure 6 shows the hypothesized subcritical bifurcation for the system, in which a "clustering metric" (vertical velocity w on the cluster scale) is used.

In preliminary attempts at a nonlinear two-layer model of RCE, updraft mass flux does show evidence of aggregation. However, it is unclear as to whether the aggregated state is a unique attractor of sorts for RCE.

Given the idealized nature of the two-layer model considered here, it is natural to ask how relevant the results obtained are. It can be seen that in a model of deep convective self-aggregation above uniform SST [Bretherton et al., 2005], aggregation dramatically dries the atmosphere (in the sense of the whole domain average), as seen in figure 7. As a result, the greenhouse effect is reduced and SST would be expected to drop, though disaggregation may not occur due to the hysteresis of the system. In considering several datasets (including

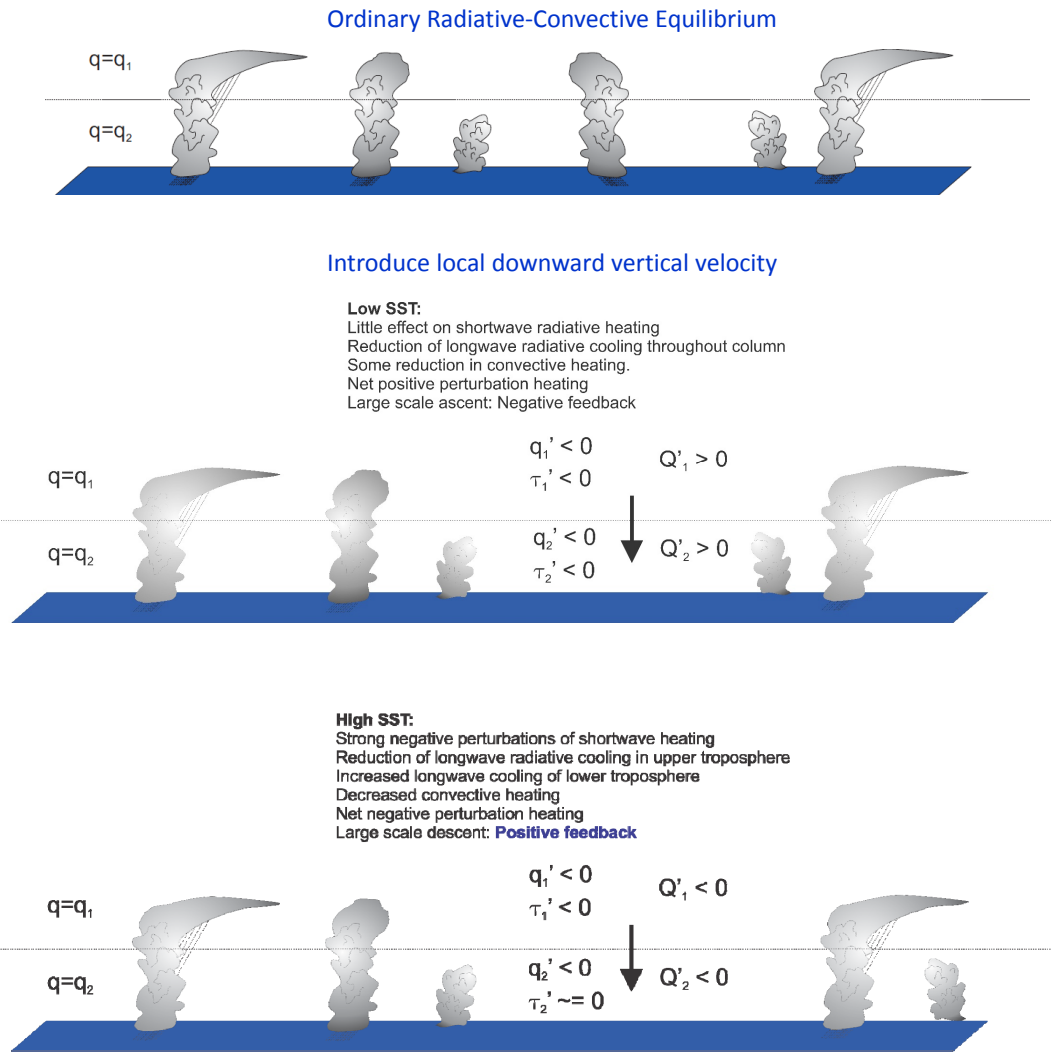

Figure 5: Response of the two-layer RCE model (top) to a local downward perturbation in vertical velocity for (middle) low SST and (bottom) high SST. (Original artwork by Kerry Emanuel.)

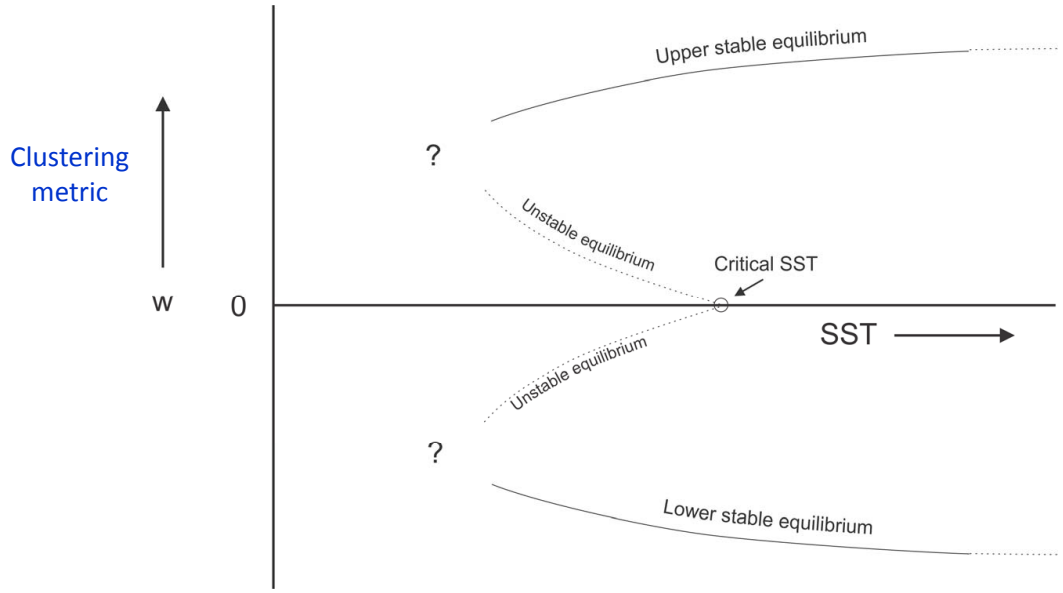

Figure 6: Hypothesized subcritical bifurcation. From figure 7 of Emanuel et al. [2014].

satellite observations and reanalysis data), Tobin et al. [2012] defined an empirical "Simple Convective Aggregation Index" (SCAI) based on the number of convective clusters and the distances between clusters. They found that the atmosphere was drier in locations where convection was more clustered.

One conjecture for the self-organization of RCE, shown in figure 8, is as follows. In cases of high SST, convection self-aggregates. However, this causes the horizontally-averaged humidity to drop dramatically, which in turn leads to a decreased greenhouse effect and cooling of the system, causing disaggregation of the convection. Thus, we can hypothesize that the system wants to be near the phase transition to the aggregated state, i.e. with SST near the critical temperature for self-aggregation.

Based on this hypothesis, we can consider a situation of "self-organized criticality", first proposed by David Neelin for a different mechanism. This proposal says that the system should reside near the critical temperature for self-aggregating, thus regulating tropical SST. In addition, the convective cluster size should follow a power-law distribution.

Several questions remain which could be asked about the two-layer RCE model:

1. How good is the assumption of convective equilibrium?
   There is a substantial amount of debate regarding this point, and the answer is, at present, unknown. However, there is some suggestion that the assumption is more justified on the macro scale, i.e. for longer scales in space and time.

2. If self-aggregation occurs on large scales, is there a breakdown of the range over which RCE exists? Might this be related to the behaviour of the Madden-Julian Oscillation?

3. Is self-aggregation seen in climate models?

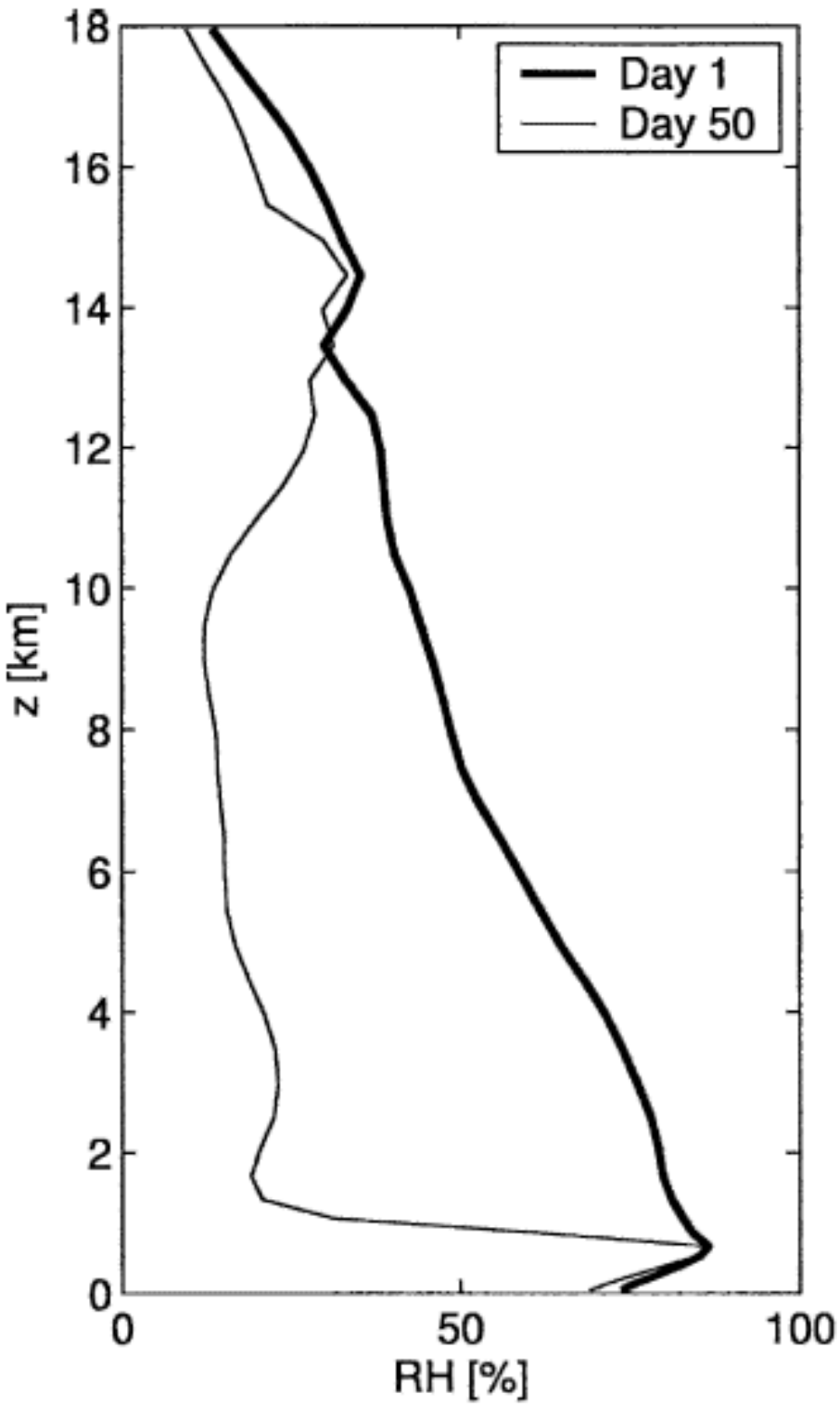

Figure 7: Horizontally averaged profile of relative humidity on day 1 and day 50 of a cloud-resolving model with self-aggregating convection. From figure 4 of Bretherton et al. [2005].

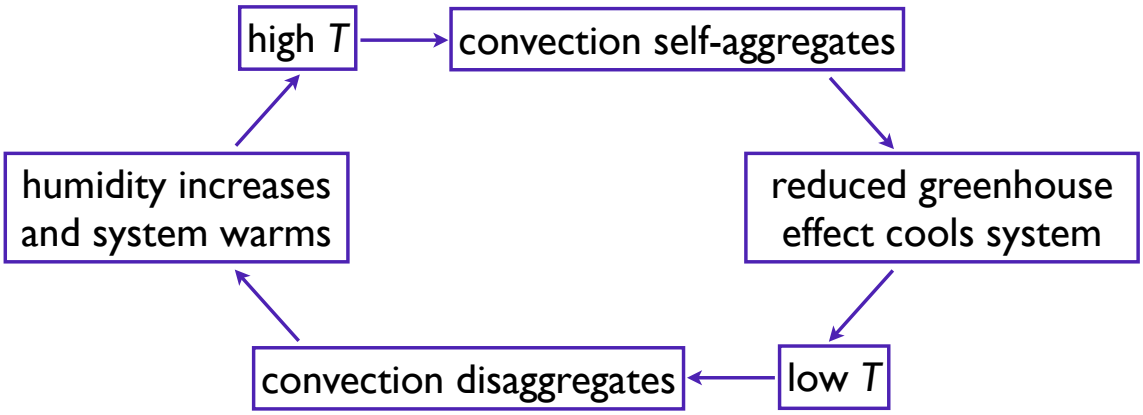

Figure 8: Hypothesis for self-organization of RCE.

Probably not, or not accurately, as there is no explicit coupling of convective downdrafts to surface fluxes, and so the necessary feedbacks are missing. However, the physics required to *maintain* clusters once initialized are there in global climate models – what is lacking are the physics need for spontaneous formation of clusters.

2 Hurricanes

In further considering the self-aggregation problem discussed above, it is natural to ask what the result would be if rotation were included. As figure 9 shows, for a 3000 km 3D box with vertically-integrated water vapour, the self-aggregated clusters appear to have become hurricanes. In figure 10, where the rotation rate has been increased, multiple smaller hurricanes are seen in the box, thereby indicating that the hurricanes have an associated size and spacing, unlike the non-rotating clusters which scaled with domain size. However, the transition temperature from the non-aggregated to aggregated states is not strongly affected by the addition of rotation.

The energy production associated with an ideal hurricane is shown in figure 11. The energetics are comparable to a Carnot cycle, in which maximum efficiency results from the particular cycle of isothermal expansion, adiabatic expansion, isothermal compression, and adiabatic compression. This is similar to what occurs in a hurricane, in which air rises due to excess enthalpy, expands, and descends. It should be noted that the last leg, however, is not adiabatic in a hurricane – while air cools radiatively, the environmental temperature profile is moist adiabatic and so the amount of cooling is equivalent to that of saturated air descending moist adiabatically. This is also shown for a real hurricane (Hurricane Inez) in figure 12. The maximum rate of energy production is

$$P = \frac{T_s - T_0}{T_s}\dot{Q} \tag{2}$$

where T_s and T_0 are the surface and outflow temperatures, respectively, and $\dot{Q}$ is the rate of heat input. The hurricane has a high-entropy core which takes heat out of the ocean. Based

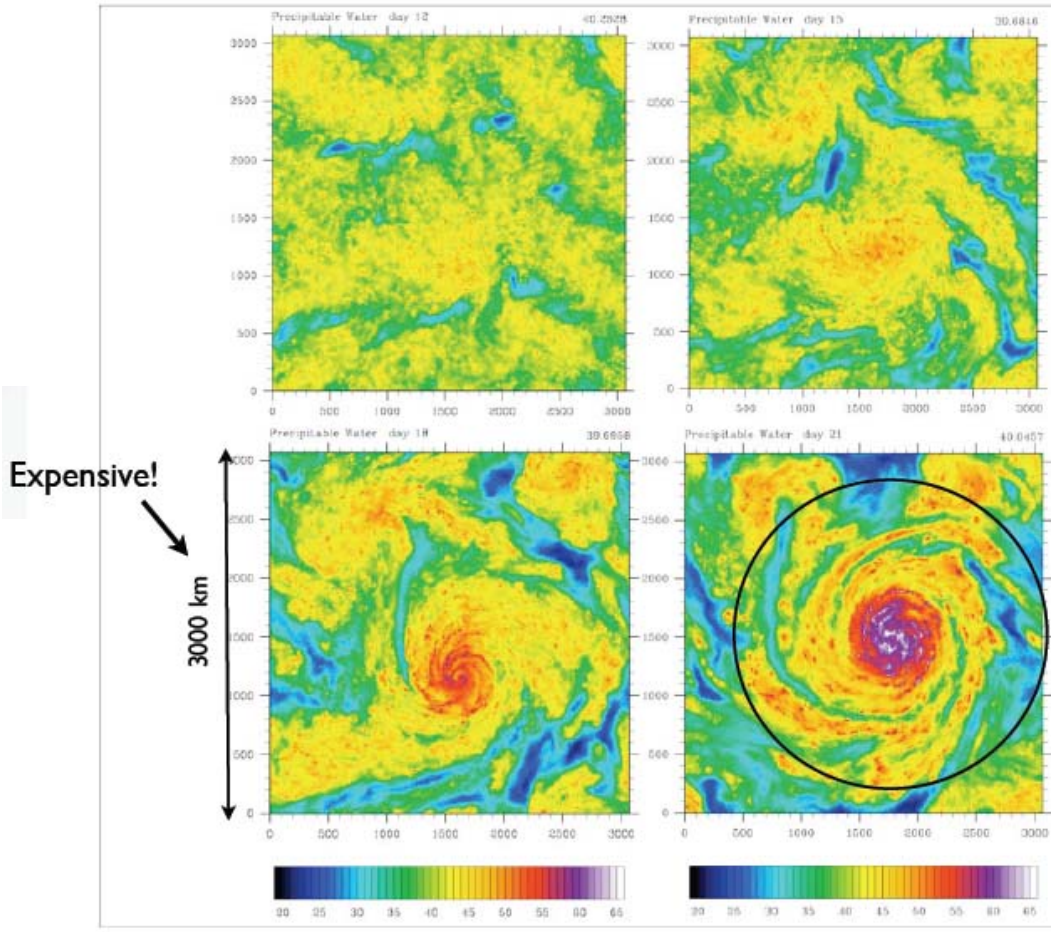

Figure 9: Several snapshots of precipitable water (days 12, 15, 18, and 21) for rotating RCE. The formation of a hurricane is indicated in the bottom right panel.

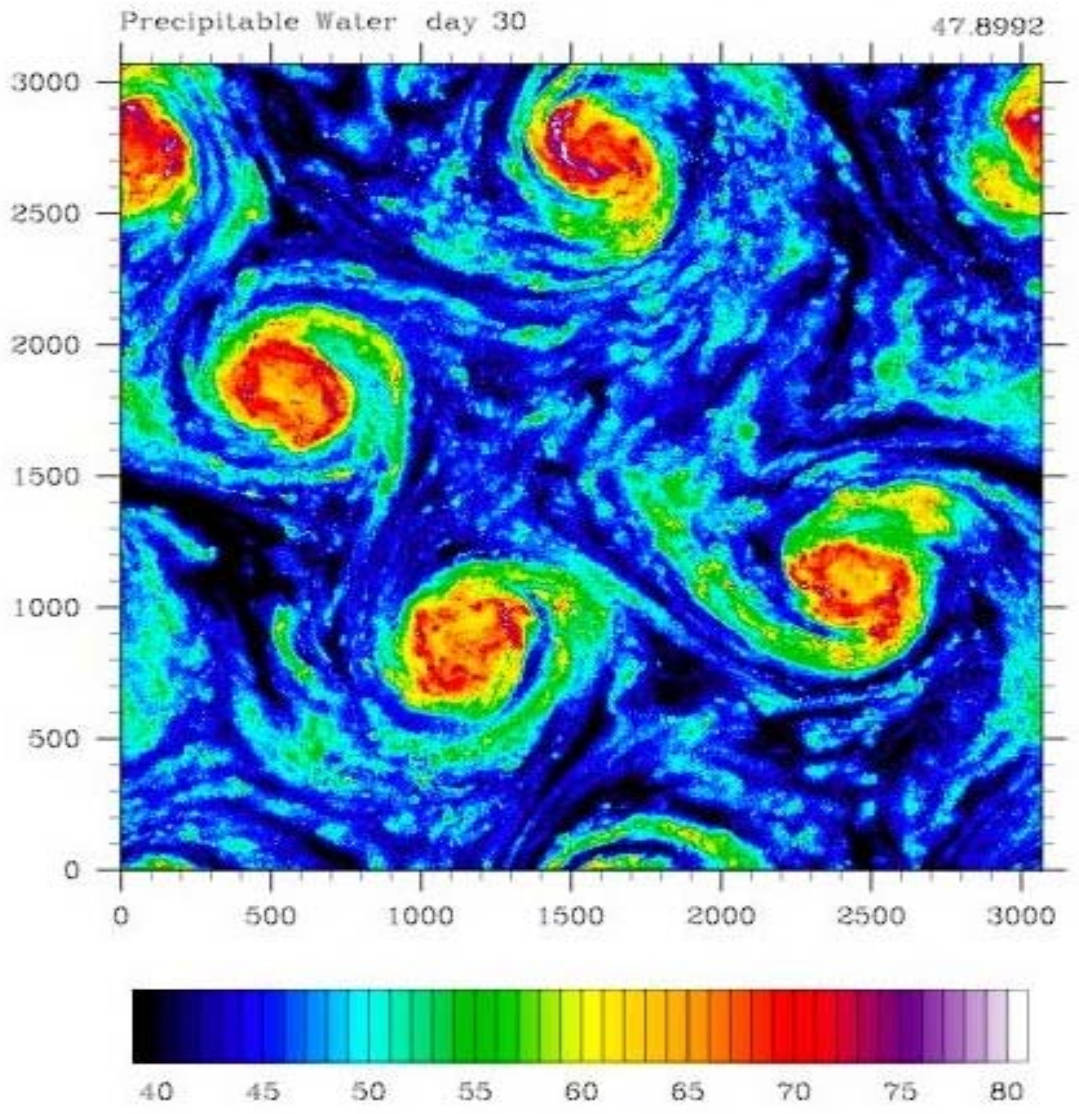

Figure 10: Snapshot of precipitable water (day 30) for rotating RCE. Here, the rotation rate f has been increased from that of figure 9.

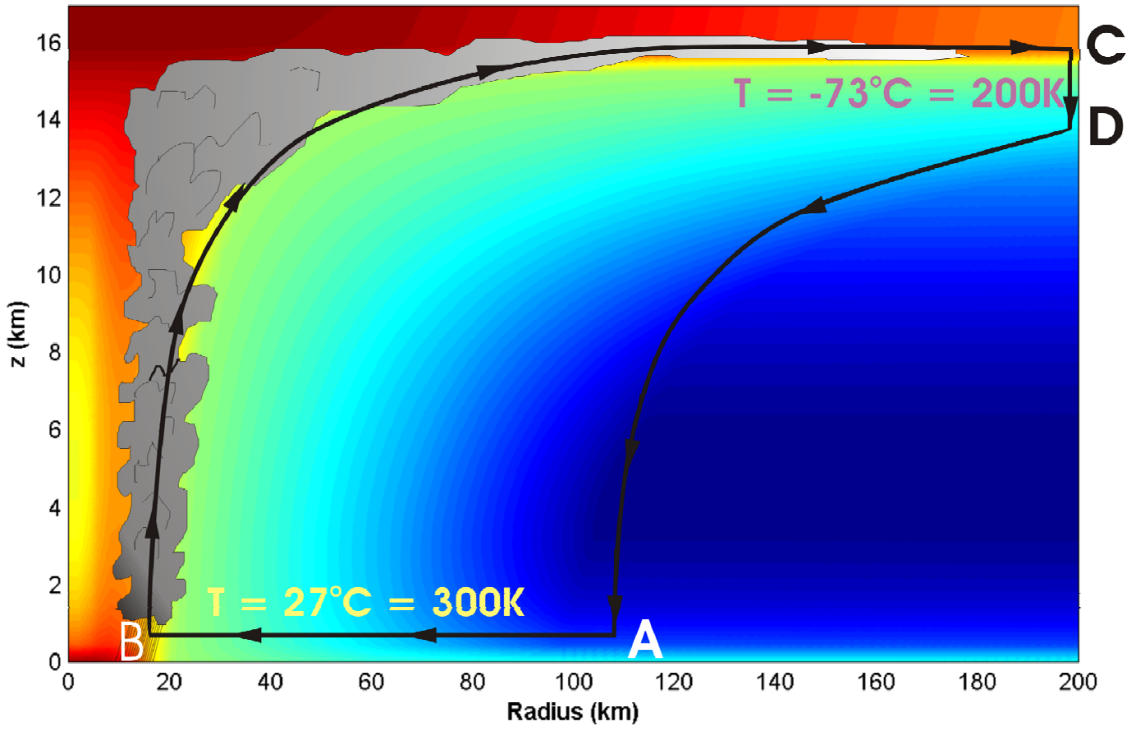

Figure 11: Energy production associated with an idealized hurricane. Red (blue) denotes regions of high (low) entropy.

on the energy cycle in figure 11, the maximum steady intensity that the storm can achieve, also known as the "potential intensity", can be computed and related to a maximum wind speed [Emanuel, 1999].

The theoretical maximum wind speed for the hurricanes can be derived as

$$|V_{pot}|^2 \simeq \frac{C_k}{C_D}\frac{T_s - T_0}{T_0}(k_0^* - k) \tag{3}$$

where C_k/C_D is the ratio of exchange coefficients of enthalpy and momentum and $k_0^* - k$ is the air-sea enthalpy disequilibrium. This air-sea enthalpy disequilibrium is the driver of hurricanes, and occurs due to the presence of greenhouse gases in the atmosphere. Using the maximum wind speed, V_{pot}, a scaling for rotating RCE can be derived.

Using the above quantities, as well as the modified thermodynamic efficiency $\varepsilon \equiv (T_s - T_0)/T_0$, angular velocity of the Earth's rotation Ω, saturation concentration of water vapour at the sea surface $q_s \sim \mathrm{e}^{T_s}$, and net upward radiative fluxes at the surface and the top of the atmosphere, F_s and F_{TOA} respectively, scalings for the hurricanes can be derived. These include the potential intensity, $V_p^3 \approx \varepsilon(F_{TOA} - F_s)/C_D$, the radius at which maximum winds occur , $r_m \sim V_{pot}/\Omega$, the distance between storm centres, $D \sim \sqrt{L_v q_s}/\Omega$ (alternately, the deformation radius), and the number density (i.e. number of storms per unit area), $n \sim \Omega^2/(L_v q_s)$.

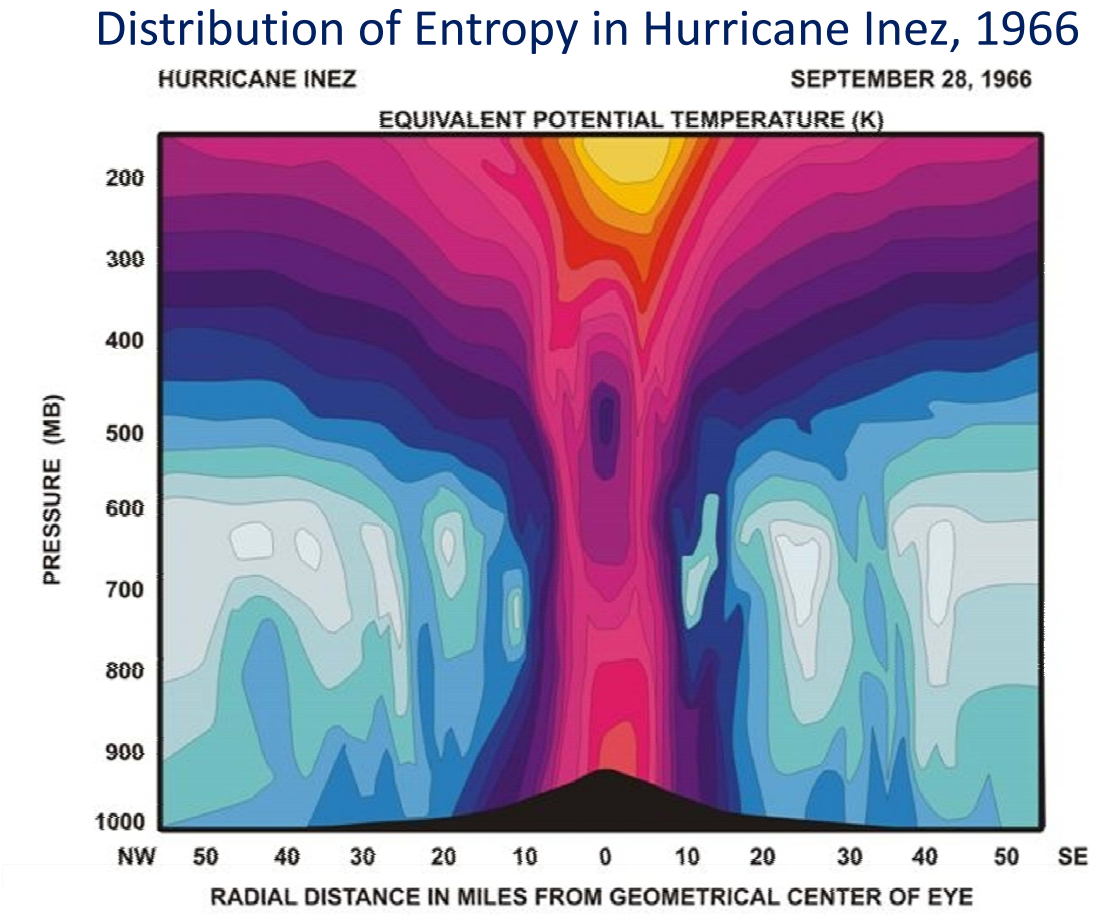

Figure 12: Equivalent potential temperature in Hurricane Inez. Graphic by Kerry Emanuel, based off of figure 6 of Hawkins and Imbembo [1976].

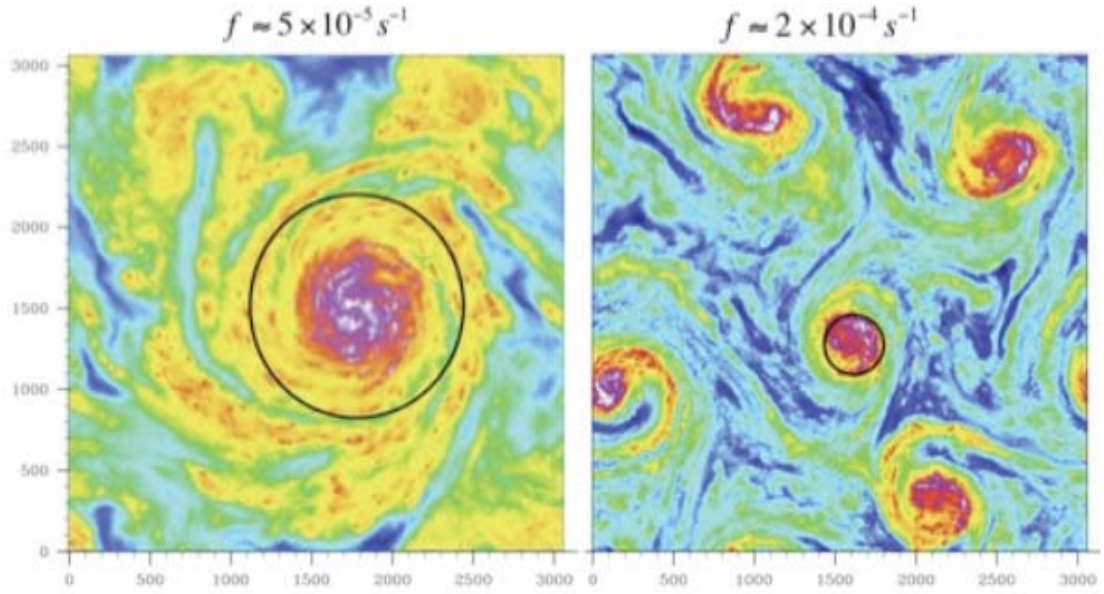

Figure 13: Snapshots of precipitable water in rotating RCE with $f \approx 5 \times 10^{-5}\,\mathrm{s}^{-1}$ (left) and $f \approx 2 \times 10^{-4}\,\mathrm{s}^{-1}$ (right). Approximate sizes from scaling analysis are indicated by the black circles. (From figure 1 of Khairoutdinov and Emanuel [2013]

Simulations agree well with this scaling. For example, figure 13 shows the result of increasing the rotation speed with the eye of storm deformation radius overlaid. The decreasing radii, increasing number density, and decreasing distance between storm centres all agree well with the predictions of the hurricane world scaling. Increasing the SST is seen to lead to fewer, but more intense, events, as shown in figure 14.

3 RCE of an Earth-like aquaplanet

The question remains of how to relate RCE with large-scale dynamics. To answer this, we can consider a hypothetical Earth-like planet without continents (i.e. an aquaplanet) or seasons, for which the only friction that acts on the atmosphere is at the surface itself. As the RCE state depends only on the latitude, we can imagine calculating the RCE state at each latitude of the planet (bearing in mind that this would lead to difficulties at the poles, for which this problem is not defined owing to the lack of radiation). While there are some rather substantial differences between Earth and the planet described here, we can compare between the real world and the hypothetical planet, asking "why do we not observe the same balance in reality?"

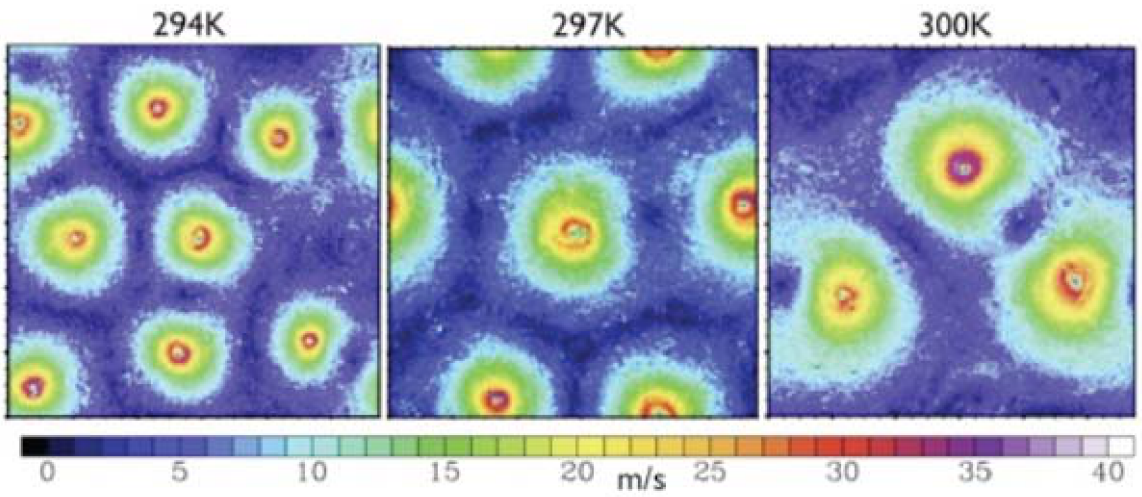

Figure 14: Snapshots of near-surface wind (m/s) in rotating RCE for three different values of SST: 294 K (left), 297 K (centre), and 300 K (right).

The primary advantage of the setup described here is that there is an *exact* nonlinear equilibrium solution for the atmospheric flow. This solution is characterized by

1. every column of the atmosphere, as well as the surface beneath it, is in RCE
2. the wind vanishes at the surface of the planet
3. horizontal pressure gradients are balanced by Coriolis accelerations
4. surface pressure is constant

The pressure above the surface decreases poleward. This decrease in pressure occurs more rapidly at higher altitudes. The pressure gradient is in geostrophic balance with a west wind, and the wind experiences a vertical shear due to the horizontal temperature gradient from incoming radiation, i.e. the system is in thermal wind balance, as shown in figure 15. The atmosphere-ocean heat flux from the equator to the poles means that there is a heat balance at the top of the atmosphere.

However, this setup does have the potential for some difficulty. For instance, it is possible that the planet does not have sufficient angular momentum to support the west-east wind required by the thermal wind balance. Also, it is possible that the equilibrium solution may be unstable. Instabilities such as baroclinic instability in mid- to high-latitudes may lead to the formation of eddies, which would in turn cause radiative imbalance, thus moving away from the thermal wind balance previously computed.

References

C. S. Bretherton, P. N. Blossey, and M. Khairoutdinov. An energy-balance analysis of deep convective self-aggregation above uniform SST. *J. Atmos. Sci.*, 62:4273–4292, 2005.

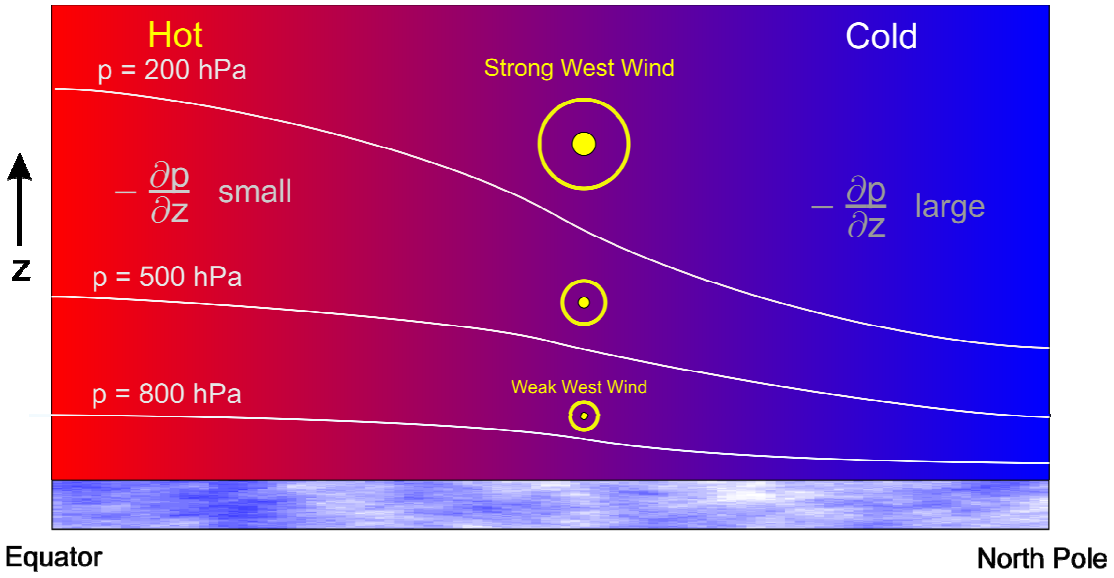

Image credit: *Kerry Emanuel*

Figure 15: Thermal wind balance for an Earth-like planet without continents or seasons. Original artwork by Kerry Emanuel.

K. Emanuel, A. A. Wing, and E. M. Vincent. Radiative-convective instability. *J. Adv. Model. Earth Syst.*, 6:75–90, 2014.

K. A. Emanuel. Thermodynamic control of hurricane intensity. *Nature*, 401:665–669, 1999.

H. F. Hawkins and S. M. Imbembo. The structure of a small, intense hurricane – Inez 1966. *Mon. Weather Rev.*, 104:418–442, 1976.

M. Khairoutdinov and K. Emanuel. Rotating radiative-convective equilibrium simulated by a cloud-resolving model. *J. Adv. Model. Earth Syst.*, 5:816–825, 2013.

J. Nilsson and K. A. Emanuel. Equilibrium atmospheres of a two-column radiative-convective model. *Q. J. R. Meteorol. Soc.*, 125:2239–2264, 1999.

D. J. Raymond and X. Zeng. Instability and large-scale circulations in a two-column model of the tropical troposphere. *Q. J. R. Meteorol. Soc.*, 124:3117–3135, 2000.

A. H. Sobel and C. S. Bretherton. Modeling tropical precipitation in a single column. *J. Clim.*, 13:4378–4392, 2000.

I. Tobin, S. Bony, and R. Roca. Observational evidence for relationships between the degree of aggregation of deep convection, water vapor, surface fluxes, and radiation. *J. Clim.*, 25:6885–6904, 2012.